PAPER

Design and experimental research on a self-magnetic pinch diode under MV

Plasma Sci. Technol. **20** (2018) 014014 (6pp) https://doi.org/10.1088/2058-6272/aa8592

Design and experimental research on a self-magnetic pinch diode under MV

Pengfei ZHANG (张鹏飞)[1,2], **Yang HU** (胡杨)[2], **Jiang SUN** (孙江)[2], **Yan SONG** (宋岩)[2], **Jianfeng SUN** (孙剑锋)[2], **Zhiming YAO** (姚志明)[2], **Peitian CONG** (丛培天)[2], **Mengtong QIU** (邱孟通)[2] **and Aici QIU** (邱爱慈)[1,2]

[1] State Key Laboratory of Electrical Insulation and Power Equipment, Xi'an Jiaotong University, Xi'an 710049, People's Republic of China
[2] State Key Laboratory of Intense Pulse Radiation of Simulation and Effect, Northwest Institute of Nuclear Technology, Xi'an 710024, People's Republic of China

E-mail: zhpf002@163.com and zhangpengfei@nint.ac.cn

Received 10 May 2017, revised 10 August 2017
Accepted for publication 10 August 2017
Published 28 November 2017

Abstract

A self-magnetic pinch diode (SMPD) integrating an anode foil-reinforced electron beam pinch focus and a small high-dose x-ray spot output was designed and optimized. An x-ray focal spot measuring system was developed in accordance with the principle of pinhole imaging. The designed SMPD and the corresponding measuring system were tested under ~MV, with $1.75 \times 2\ mm^2$ oval x-ray spots (AWE defined) and forward directed dose 1.6 rad at 1 m. Results confirmed that the anode foil can significantly strengthen the electron beam pinch focus, and the focal spot measuring system can collect clear focal spot images. This finding indicated that the principle and method are feasible.

Keywords: plasma, pulsed x-ray flash radiography, self-magnetic pinch diode

(Some figures may appear in colour only in the online journal)

1. Introduction

Pulsed x-ray flash radiography can determine the relevance of the structure, state and evolution of objects at high-velocity motion, and this technique plays an important role in national defense and civil fields. The high-current pinch diode has been extensively investigated in many countries, since the Sandia National Laboratories of the United States conducted a series of flash radiography experiments to diagnose the detonation hydromechanics properties of materials with rod pinch diode technology (Cygnus device) [1, 2]. Related institutions have also conducted theoretical and applied research on high-current radiographic diodes, such as self-magnetic pinch, rod pinch, plasma-filled rod pinch and paraxial diodes.

Rod pinch diodes are limited by the spatial distribution characteristics of the radiation field and are often used in an environment where voltage is not higher than 6 MV [3–6]. A plasma filled rod pinch diode, which exhibits low impedance, is applicable to low working voltages (1–2 MV) [7, 8]. Paraxial diodes are disadvantageous because of their complicated structure and large focal spots (diameter = 4–6 mm), and their impedance is than that of rod pinch or self pinch diodes [9]. Self-magnetic pinch diodes (SMPD), which can achieve high radiation dosage (hundreds of rad) and small focal spots (approximately 2 mm) at high voltages (>10 MV), have been examined in current theoretical and application studies to satisfy the requirements of flash radiography for thick materials with high atomic numbers [10–15].

AWE (Atomic Weapons Establishment) examined the principle of SMPD on a prototype IVA module (PIM) accelerator, investigated the effects of the structural parameters of SMPD on radiation dosage and focal spot size at 1–3 MV, and obtained 2–5 mm focal spots and 4–10 rad at 1 m [10, 11]. In 2003, the diode structure was optimized, SMPD was driven by Mogul D, and 54 rad at 1 m and 2.1 mm focal spots were obtained at 4.2 MV. Sandia National Laboratories in the United States tested SMPD on RITS-6 at high voltages (6.5 MV), achieved 350 rad at 1 m and 2.9 mm focal spots, and focused on the impedance stability of SMPD [12–14].

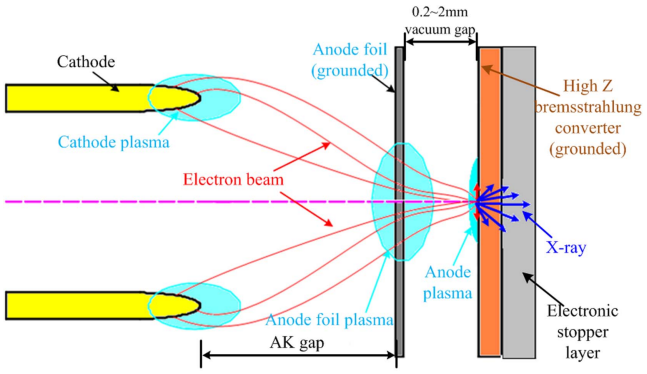

Figure 1. Operation of the SMPD.

In previous experiments, SMPD collected high-quality x-ray spots and radiation parameters; thus, this technology can be applied to flash radiography. Therefore, this study designed and optimized the mechanical structure of diodes that could be easily assembled and could ensure installation accuracy and consistency. A pinhole imaging system for focal spot diagnosis was also developed. The designed SMPD and pinhole imaging system were verified through experiments based on the 'Chenguang' accelerator (1 MV, 40 kA, and 40 ns).

2. Design and optimization of the SMPD structure

SMPD achieves a strong pinch of electron beam based on the self-magnetic field of the beam and the anode plasma produced during the operation. The typical structure and working principle of SMPD are shown in figure 1. At a high-voltage electric pulse, the field intensity on the cathode surface of the SMPD exceeded the field emission threshold of the material, and the tapering cathode emitted electron beams. With the self-poloidal magnetic field, the electron beams converged to the center at a range of deflection angles. As a result, high-intensity pinch electron beams were formed. The red curves in figure 1 represent electron orbits. High-energy electron beams hit the anode foil and formed dense anode foil plasma in the anode foil region before the converter. On the one hand, these electron beams were driven by the magnetic field force to pinch toward a smaller converter region when the plasma was dense enough to shield the electric field on the anode surface. On the other hand, ions from the anode foil plasma accelerated to move to the cathode, and the ion current further intensified the pinch effect of the electron beams. The strong pinching of the electron beams on the converter behind the anode foil could form small focal spots. High-energy electron beams hit the high Z bremsstrahlung converter, and bremsstrahlung created small x-ray point sources.

Figure 2 shows the structure of a typical SMPD. The annular cathode was composed of high-density graphite, and its outer diameter was about 10 mm, with a rounding corner angle at the end. Evident material defects and structural changes should be avoided to maintain a uniform electric field and achieve initial uniform electron emission. The vacuum

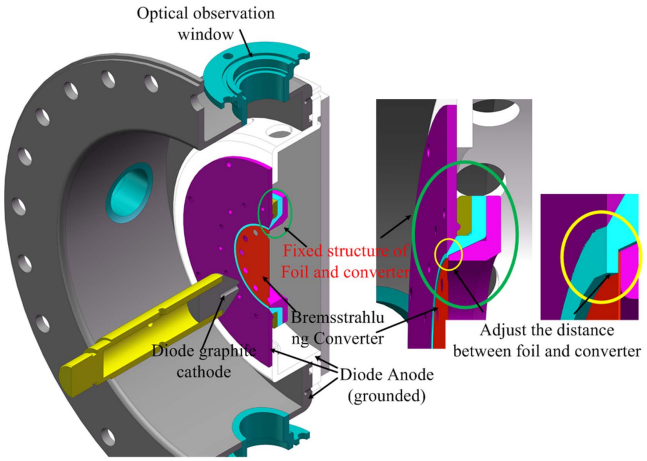

Figure 2. Structure of SMPD (anode foil is disregarded).

gap found at the anode of the SMPD was used as the base of the anode foil and the converter, which was also the anode backflow structure of the whole diode. Quartz glass windows were set surrounding the vacuum gap for the convenience of optical observation during the SMPD operation.

The anode foil consisted of a 12 μm thick Mylar layer with a 1 μm thick metal coating on both sides. With good tenacity and appropriate stretching, the Mylar film could tightly and completely cover the whole surface. This film was fixed by two metal rings in which a semicircular seam allowance was provided to protect the structure from uniform stress and strong fixation of the Mylar film. Metal rings matching the slope were placed behind the anode foil to stretch it tightly and to keep it flat. The distance between the anode foil and the converter is a key parameter of SMPD structural design. This parameter generally ranges between 0.2 mm and 2 mm, but it can be adjusted accurately. Therefore, platforms with different thicknesses were installed on the inner circle of the tensioning ring flange to adjust the distance between the anode foil and the converter. Finally, air-bleed holes were designed at the peripheral anode converter to maintain a high vacuum space between the anode foil and the converter.

3. Pinhole imaging system for x-ray focal spot measurement

3.1. Structure design

To evaluate the key parameters, such as size, of x-ray spots produced by SMPD [15], we designed a focal spot measuring system according to the principle of pinhole imaging. This pinhole device with high spatial resolution and a high-efficiency image detection system was needed to measure 2–5 mm x-ray spots. The energy of x-rays produced by SMPD was ~MeV, and x-rays were strongly penetrating. Therefore, a coarse pinhole (diameter = 0.3 mm) structure was used for imaging, and rear-end images were collected with an image plate (IP), which can be read and written repeatedly. The x-ray spot was amplified using a coarse

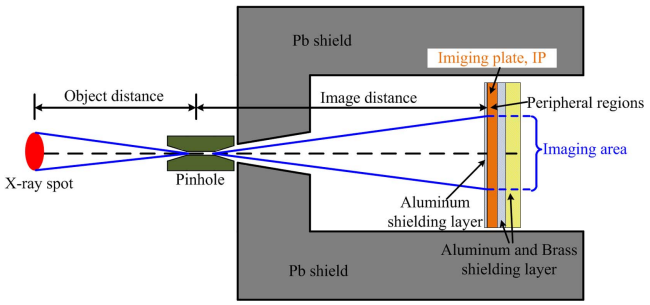

Figure 3. Measuring system of x-ray spot.

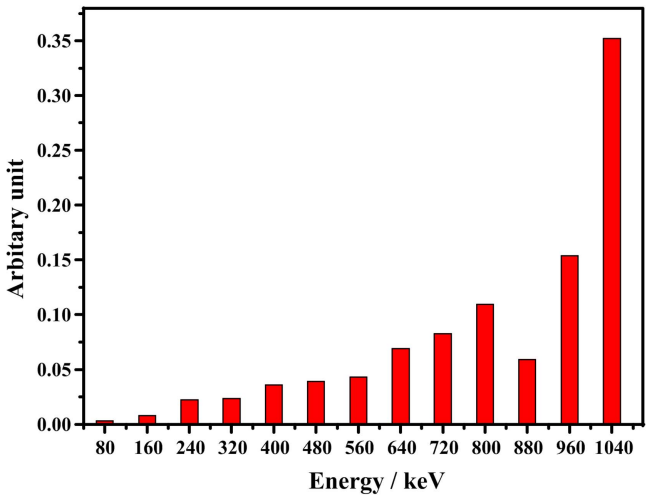

Figure 4. Energy spectral distribution of electron beams.

pinhole and projected onto the IP. The image size on the IP and the x-ray spot satisfied the proportional relation of geometrical optics, which was determined by the 'distance between the spot image and the pinhole' and the 'distance between the pinhole and IP.' These two distances were easily measured after the measuring system was debugged.

IP sensed light through a BaBrF material, x-ray interacted with BaBrF on the IP, and the x-ray intensity image was converted into a corresponding visible image. An exponential relationship existed between the image brightness on the IP and the irradiation dose in the imaging area. The imaging area of the IP was 10 in$\times$12 in, and the single pixel size (spatial resolution) was 0.1 mm $\times$ 0.1 mm. The IP was placed in an enclosed cavity filled with Pb masses and thus prevented light sensing caused by x-ray scattering. The whole measuring system is shown in figure 3.

With limited space, the distance between the converter and the pinhole was 27 cm. To maintain an adequate spatial resolution of the measuring system, we set the distance between the pinhole and the IP to 54 cm and the imaging amplification factor of the pinhole to 2. SMPD spots were estimated to be 2–5 mm circular spots, which could control the image size on the IP within 4–10 mm and at least 1,000 pixels in the spot region for sampling. Limited by conditions, the discharge shake of the experimental preparation and the device generator may cause centering misalignment of the imaging system. Therefore, the pinhole centering must be adjusted for each experiment. This adjustment shows that the proportional relationship between a focal spot and an image is determined by the measured distance between the pinhole and the converter and the distance between the pinhole and the IP before the experiment. The data in the following text included the spot size calibration of the proportionality coefficient, and these data were normalized according to the size at the origin spot.

3.2. Simulation of photon transportation in the pinhole imaging system

Low-energy rays formed by high-energy x-ray scattering in a shield space possibly cause adverse effects on measuring systems and yield a high-energy deposition efficiency on IP. Therefore, they can easily cause overexposure of IP or heavy exposure of regions beyond the imaging area and consequently induce exposure saturation of IP or produce a low contrast ratio. However, these results are inconsistent with image acquisition and analysis. Aluminum plates were coated tightly on the front and back surfaces of the IP to shield low-energy x-rays. A Monte Carlo model of the pinhole imaging system was established to analyze energy deposition in the imaging area and peripheral regions quantitatively. In the numerical model, the energy spectra of electrons were estimated according to voltage and current on SMPD. The time integral of the current represents the number of electrons. If voltage changes slightly within a certain period, then this parameter is fixed and the integral of the current in this period can be used to calculate the number of electrons, that is, the number of electrons at a specific voltage. Hence, electron sources may be distributed linearly (2 mm long) and may hit the converter normally. The energy distribution when electron beams arrived at the anode surface under voltage and current waveforms is shown in figure 4. Voltage and current pulse exhibit similar variation trends and simultaneously reach the peak. Therefore, high energy accounts for a large proportion in the electron beam spectra.

The Monte Carlo model was established on the basis of the SMPD structure and spatial layout of the measuring system in figure 3. The electron beams hit the 0.2 mm thick Ta target supported by a piece of 8 mm thick organic glass cover-plate at about 10 cm behind. The pinhole structure and the tapered Pb shield were successively set behind the glass window. The Pb shield consisted of a pre-positioned aluminum shielding layer, an IP, and a post-positioned brass shielding layer. A thick metal shielding layer was applied because the brass shielding layer behind the IP only shielded the scattered rays to improve image contrast between the imaging area and the peripheral regions. The post-positioned metal layer comprised a composite structure of a piece of 2 mm aluminum layer and a piece of 5 mm brass layer. The pre-positioned metal layer contained a 1 mm thick aluminum layer. The spatial distribution of energy deposition on IP is shown in figure 5. The energy deposition in the imaging area was dozens of times higher than that in the peripheral regions. An evident 'halo' was found approximately in the 1 mm circular region within the peripheral regions (two

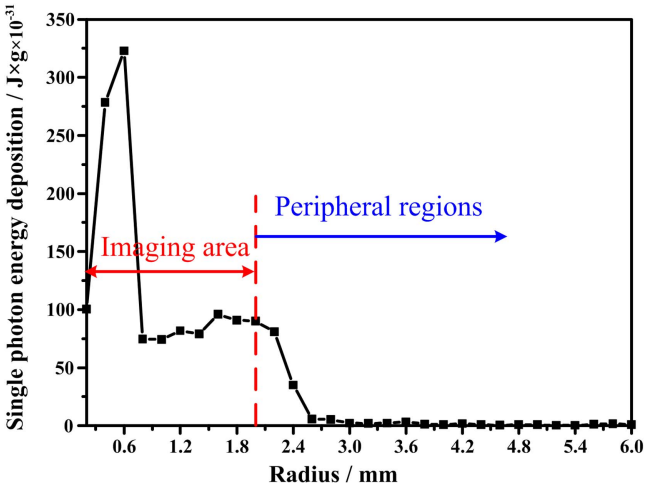

Figure 5. Spatial distribution of single photon energy deposition on IP.

magnification times and 2 mm away from the center) because x-ray spots are spatially distributed to a greater extent than a strict point source.

4. Experimental results and analysis

4.1. Experimental results under different structural parameters of SMPD

The focus characteristics of SMPD under MV and a pulsed x-ray spot measuring system based on the pinhole imaging system were examined on the 'Chenguang' accelerator. Developed in 1988, the 'Chenguang' accelerator could choose the transmission line for driving oil media to obtain a high-voltage output (1–2 MV) and the transmission line for driving water media to obtain a large current output (approximately 100 kA). The Marx generator includes a total of 24 levels and adopts a symmetric charge mode. The capacitance and withstanding voltage of each level are 40 nF and 100 kV, respectively. The total capacitance and total energy storage of the Marx generator are 1.67 nF and 4.8 kJ. The generator contains 12 spark switches: the first four switches are for TG70 triggering and the remaining switches are for overvoltage-based self-breaking. In this experiment, oil media line was chosen to adjust the charging voltage of the Marx accelerator, and approximately 1 MV pulsed voltage was obtained stably on the load of SMPD.

In the experiment, the distance between the anode foil and the converter was fixed at 0.75 mm, and the distance between the graphite cathode and the anode foil could be adjusted between 5 mm and 45 mm. We conducted three experiments under three typical states. (1) The distance between the anode and cathode of the SMPD was 19 mm, and the anode contained one piece of 0.2 mm thick Ta target. No anode foil was placed between the Ta target and the cathode. Typical experimental results are shown in figure 6 (Shot2016031701). (2) The distance between the anode and the cathode of the SMPD was 32 mm, and the anode included one piece of 0.2 mm thick Ta target. A piece of 13 μm thick aluminum coated with a Mylar film was used as the anode foil between the converter and the cathode. The distance between the anode foil and the converter was 0.75 mm. Typical experimental results are shown in figure 7 (Shot2016031601). (3) The third structure was similar to the second one except that the distance between the anode and the cathode was 18 mm (Shot2016031602), Typical experimental results are shown in figure 8. A comparison of the SMPD structures and working conditions under the three states is shown in table 1.

The anode foil and the converter after the experiments are presented in figure 9. Large-scale vaporization occurred on the anode foil because of the impact of electron beams. After the electron beams hit the converter, energy deposition sharply increased the temperature in a small region of the converter. Thus, the metal material vaporized. The thermal shock wave formed through material vaporization spraying pierced through the converter.

4.2. Effect of anode plasma on focal spot formation

The experimental results of SMPD with and without an anode foil were compared. The relative intensity of the x-ray spot images was significantly higher than that without anode foil and evidently concentrated in a region when an anode foil was used. This finding indicated that the anode foil effectively enhanced the pinching process of the electron beams and was conducive to the formation of small x-ray spots. For SMPD without an anode foil, the drop points of the electron beams on the anode target surface were less concentrated. According to the analysis, the different pinching states of the electron beams were the consequence of the differences of anode plasma. SMPDs with and without the anode foil employ significantly different mechanisms of plasma production. For the SMPD with the anode foil, anode plasma was formed through energy deposition, vaporization, and ionization after the electron beams hit the anode foil. For the SMPD without the anode foil, anode plasma was formed through the desorption of adsorbed gases after the anode Ta target was hit by electron beams. These two different production mechanisms of anode plasma led to significant differences in the distribution and parameters of plasma. The x-ray spot image of the SMPD with the anode foil showed a regular circular area, whereas the image of the SMPD without the anode foil was irregular possibly because of different spatial distributions of anode plasma. On the basis of particle simulation, Reference [10] discovered that the electron beam cannot form an effective pinch if no plasma is generated in the anode region and if the diode possesses electron beams. The parameters of anode plasma would also directly influence the pinch quality of the electron beams, as confirmed by our experiments. The x-ray spots presented random and irregular shapes because of the great randomness of plasma parameters, such as spatial distribution and production time, in the SMPD without the anode foil.

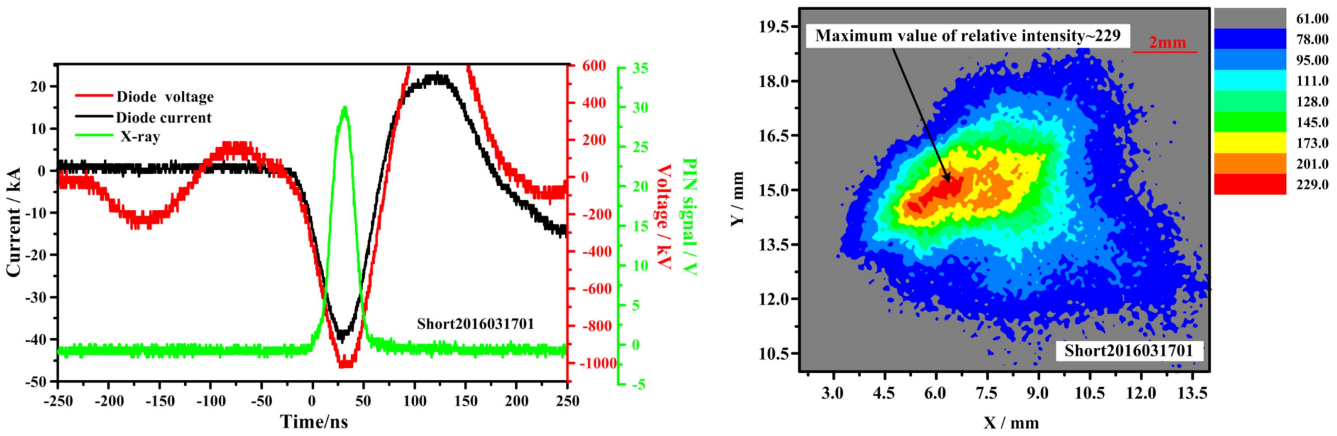

Figure 6. Working voltage, current, pulsed x-ray waveform, and focal spot images of the SMPD (Shot2016031701, AK gap = 18 mm, no anode foil).

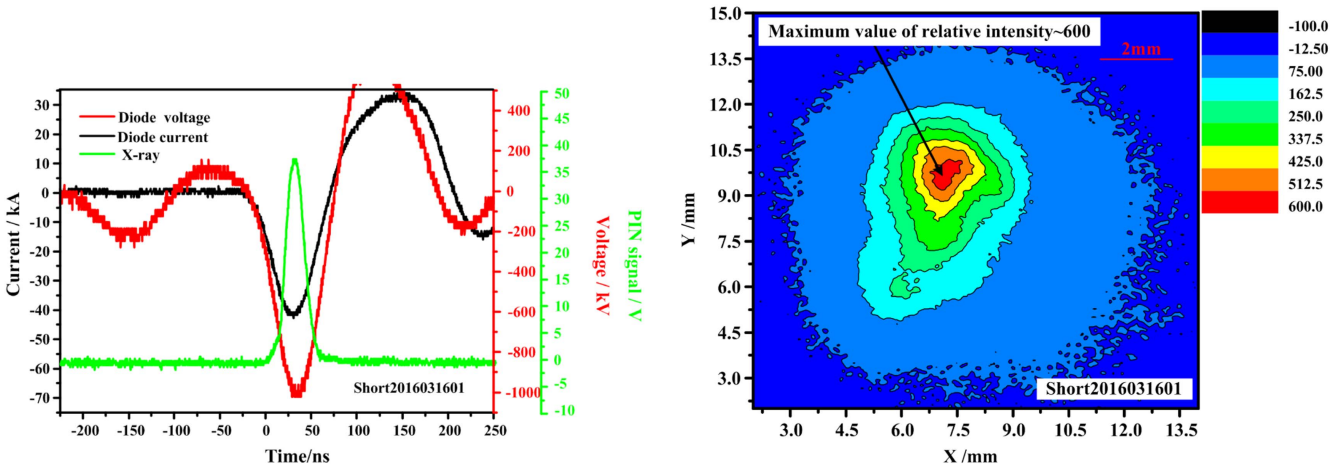

Figure 7. Working voltage, current, pulsed x-ray waveform, and focal spot images of the SMPD (Shot2016031601, AK gap = 32 mm, with anode foil, distance between the anode foil and the converter = 0.75 mm).

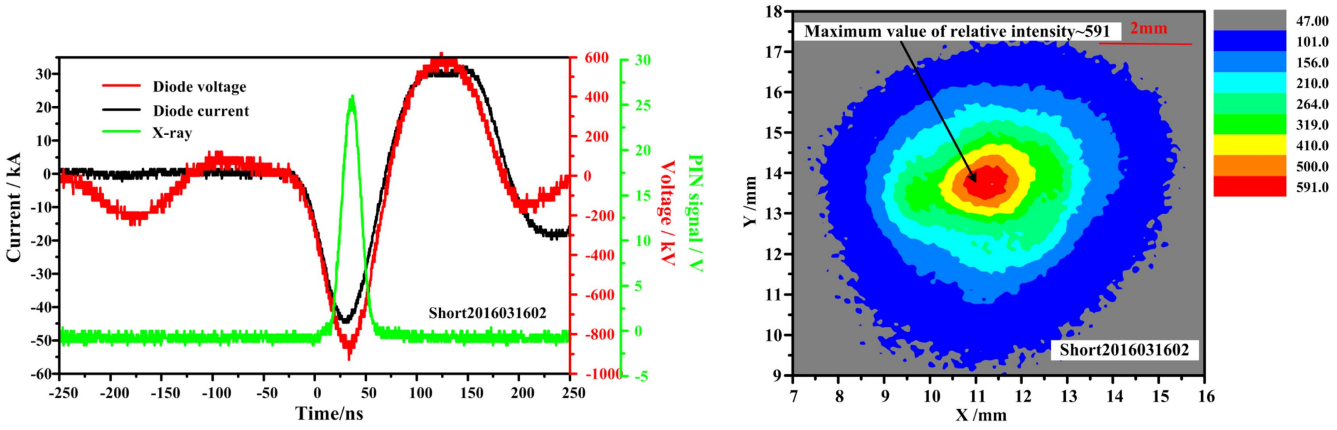

Figure 8. Working voltage, current, and pulsed x-ray waveform of the SMPD as well as images of the anode foil, the converter, and spot images (Shot2016031602, AK gap = 18 mm, with anode foil, distance between the anode foil and the converter = 0.75 mm).

4.3. Dose distribution of focal spot area

The x-ray spots in figures 6–8 revealed that the established pinhole photography matches well with the pulsed x-ray spots produced by SMPD, and the acquired images comprised clear outer boundaries and adequate resolutions. The relative intensity ratio of the imaging area and peripheral regions could reach as high as approximately 60 when the SMPD with the anode foil formed a good pinch, and this ratio was adequate to read and recognize the details of x-ray spot images. In terms of the SMPD without the anode foil, the central region of x-ray spots yielded a low relative intensity

Table 1. Comparison of different SMPD structures and working conditions.

Shot	2016031701	2016031601	2016031602
Diode voltage (MV)	1.01	1.01	0.85
Diode current (kA)	40.73	42.57	45.3
FWHM (ns)	49	50	48
Presence of anode foil	NO	YES	YES
AK gap (mm)	18	32	18
Impedance of the peak power point (Ω)	24.86	23.76	18.87
Spot size (mm)	4.3 × 2.2	3.8 × 2.6	2.0 × 1.75
Dose@1 m/rad	2.70	3.12	1.60

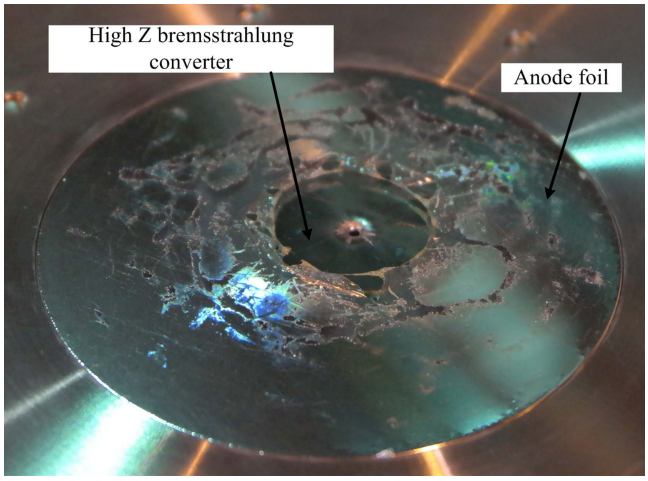

Figure 9. Image of the anode foil and the converter after experiments (Shot2016031602).

because of the scattered electron beams. The relative intensity of the imaging area was several times higher than that of the peripheral regions possibly because of two aspects. On the one hand, the drop points of electron beams in the absence of an anode foil were scattered and unable to create a distinct and strong focus. On the other hand, the pinhole image structure easily produced a larger-scaled 'halo' because of the large focusing scope, and this halo decreased the image contrast.

5. Conclusions

In this study, an SMPD with a compact structure and a high assembly accuracy is designed, and a focal spot measuring system based on pinhole imaging is developed. The designed SMPD is examined on the basis of the 'Chenguang' accelerator at ∼MV. Our results reveal that an anode foil can significantly enhance the pinch effect of electron beams. Moreover, the designed pinhole imaging system can be used to observe x-ray spots. At approximately 1 MV working voltage, the SMPD can obtain 2.0 mm (length) × 1.75 mm (width) oval spots, and the radiation dosage at 1 m reaches 1.6 rad. These findings indicate the potential of SMPD in hydrodynamics experiment. The developed focal spot measuring system, which comprises a simple structure, exhibits strong resistance to radiated interference, and displays high resolution, can stably obtain key spot parameters, including size and intensity distribution. Future studies will focus on the interaction between electron beams and plasma and will optimize SMPD to obtain smaller x-ray spots and higher radiation dosage output than those presented in our study.

Acknowledgments

The authors thank Guzhou Song, Jiahui Yin, Zhaofeng Su, Yuan Zhang, and Nan Xiang for their tireless operations in the Chenguang facility. The work was supported by National Natural Science Foundation of China (Grant Nos. 11305128 and 11505142) and the State Key Laboratory of Intense Pulsed Radiation Simulation and Effect (Grant No. SKLIPR.1503).

References

[1] Smith J *et al* 2005 Cygnus performance in subcritical experiments *IEEE 15th Int. Pulsed Power Conf. (PPC) (Monterey, CA)*
[2] Smith J *et al* 2007 Cygnus beam radiography source *IEEE 16th Int. Pulsed Power Conf. (PPC) (Albuquerque, NM)*
[3] Welch D R *et al* 2001 *Nul. Mech. Phys. Res.* A **464** 134
[4] Rose D V *et al* 2001 *J. Appl. Phys.* **91** 3328
[5] Menge P R *et al* 2003 *Rev. Sci. Instrum.* **74** 3628
[6] Satyanarayana N *et al* 2014 *Rev. Sci. Instrum.* **85** 096107
[7] Weber B V *et al* 2008 *IEEE Trans. Plasma Sci.* **36** 443
[8] Weber B V *et al* 2004 *Phys. Plasmas* **11** 2916
[9] Birrell A R *et al* 2000 *IEEE Trans. Plasma Sci.* **28** 1660
[10] Martin P N *et al* 2011 *IEEE Trans. Plasma Sci.* **39** 1943
[11] Clough S *et al* 2007 Investigation of the self magnetic pinch diode on PIM as aradiographic source *IEEE 15th Int. Pulsed Power Conf. (PPC) (Monterey, CA)*
[12] Hahn K D *et al* 2010 *IEEE Trans. Plasma Sci.* **38** 2652
[13] Bennett N *et al* 2015 *Phys. Plasmas* **22** 033113
[14] Bennett N *et al* 2014 *Phys. Rev. ST Accel. Beams* **17** 050401
[15] Li J *et al* 2009 *Rev. Sci. Instrum.* **80** 063106